Available online at www.sciencedirect.com
ScienceDirect
Trans. Nonferrous Met. Soc. China 22(2012) 2164−2170
Transactions of Nonferrous Metals Society of China
www.tnmsc.cn

Buckling pattern of TiO_2 nanotube film

ZOU Jian-peng[1], WANG Ri-zhi[2]

1. State Key Laboratory of Powder Metallurgy, Central South University, Changsha 410083, China;
2. Department of Materials Engineering, University of British Columbia, Vancouver BC, V6T 1Z4, Canada

Received 27 August 2011; accepted 10 January 2012

Abstract: Substrate straining test was carried out to study the buckling pattern of TiO_2 nanotube film. The results show that the tensile strains of buckling occurrence of TiO_2 nanotube films without annealing, with 250 °C annealing and with 400 °C annealing are 2.5%, 8.9% and 7.8%, respectively, which indicates the modifying effects of temperature annealing. Through the SEM observation, the critical buckling stresses of TiO_2 nanotube films without annealing, with 250 °C annealing and with 400 °C annealing can be estimated as 180.4, 410.2 and 619.5 MPa, respectively. The critical buckling stress of TiO_2 nanotube films with 250 °C annealing from AFM observation is estimated as 470.2 MPa, which indicates good agreement with the critical buckling stress from SEM observation. The true stress and the critical energy release rate of TiO_2 nanotube film with 250 °C annealing are given as 840.3 MPa and 77.2 J/m^2, respectively. Excellent agreement of the critical energy release rate of TiO_2 nanotube film with 250 °C annealing in terms of buckling perspective and crack perspective is obtained.
Key words: TiO_2 nanotube; anodization; buckling; energy release rate

1 Introduction

Interfacial properties for film/substrate systems can be studied on the basis of interfacial shear lag model, which was proposed by AGRAWAL and RAJ [1]. Important parameters including interfacial shear strength, energy release rate and fracture toughness can be investigated through this method. The ultimate shear strength of a metal−ceramic interface has been measured as 0.56−1.67 GPa by depositing 60 nm films of silica on pure copper substrates [1]. The energy release rate of hard and brittle Cr coating on ductile steel substrate was estimated as 57.7 J/m^2 and the estimation was consistent with the theoretical analysis and prediction presented in Ref. [2]. The interfacial shear strength of sol−gel derived fluoridated hydroxyapatite coatings on Ti6AlV substrates was measured by the shear lag method to increase from pure hydroxyapatite of 393 MPa to 459 MPa [3].

Buckling is another pattern accompanying the crack propagation during the substrate straining test. The presence of cracks not only gives rise to tensile stress relaxation, but also induces compressive stress in the perpendicular direction, which eventually leads to film buckling [4]. During the buckling process, a sequence comprising buckling occurrence, buckle propagation and spalling has been revealed [5]. Buckling at a bifurcation point of the delaminated region, resulting from incompletely relieved stresses in this region, was analyzed by a semi-analytical approach for delamination of infinite extent [6]. Buckling occurs once the compressive strength around the delamination exceeds a critical value σ_c [7]. Atomic force microscopy (AFM) is particularly suited to analyze the fine structure of buckling on a nanometer scale at the first stage of buckling since the AFM applied force used for imaging the sample surface is 10−100 nN and prevents thin films from being damaged during the analysis process [8−10].

In this work, TiO_2 nanotube films with different tensile strains after substrate straining tensile test were investigated by SEM. AFM was particularly carried out to study the small blister phenomenon (first buckling stage) of TiO_2 nanotube film with buckling occurrence strain. As far as we know, the buckling pattern study of TiO_2 nanotube film made here has not been reported so far and this study could be envisaged to be useful for

Foundation item: Project (51274248) supported by the National Natural Science Foundation of China; Project (20110946Z) supported by State Key Laboratory of Powder Metallurgy, China
Corresponding author: WANG Ri-zhi; Tel: +1-604-822-9752; E-mail: rzwang@mail.ubc.ca
DOI: 10.1016/S1003-6326(11)61444-1

understanding the fundamental aspects associated with interfacial characteristics of TiO_2 nanotube film.

2 Experimental

Pure annealed titanium foil (size 30 mm×30 mm, thickness 0.25 mm) bought from Goodfellows Co. was used in this study. With mechanical processing, the foil was cut into tensile test samples. Grinding and polishing were used to get rid of stress concentration of the tensile test samples. The thickness of polished Ti samples was controlled as (0.22±0.02) mm. The TiO_2 nanotube fabrication and temperature annealing technique followed the protocol of our previous research paper [11]. Tensile tests for the TiO_2 nanotube film were carried out on a miniature material testing machine (MINIMAT, Rheometic Scientific Co.). The strain rate was controlled as 0.1 mm/min. HITACHI S−3000N SEM was used to observe the microstructure of buckling of TiO_2 nanotube film. A DI Nanoman VS atomic force microscope was used to investigate the initial stage of buckling of TiO_2 nanotube film.

3 Results and discussion

3.1 SEM buckling observation of TiO_2 nanotube film

Buckling evolution of the TiO_2 nanotube film without annealing during the tensile test is shown in Fig. 1. The buckling initiation is at 2.5% strain and the buckle saturation is at 3.8% strain. Once the buckling

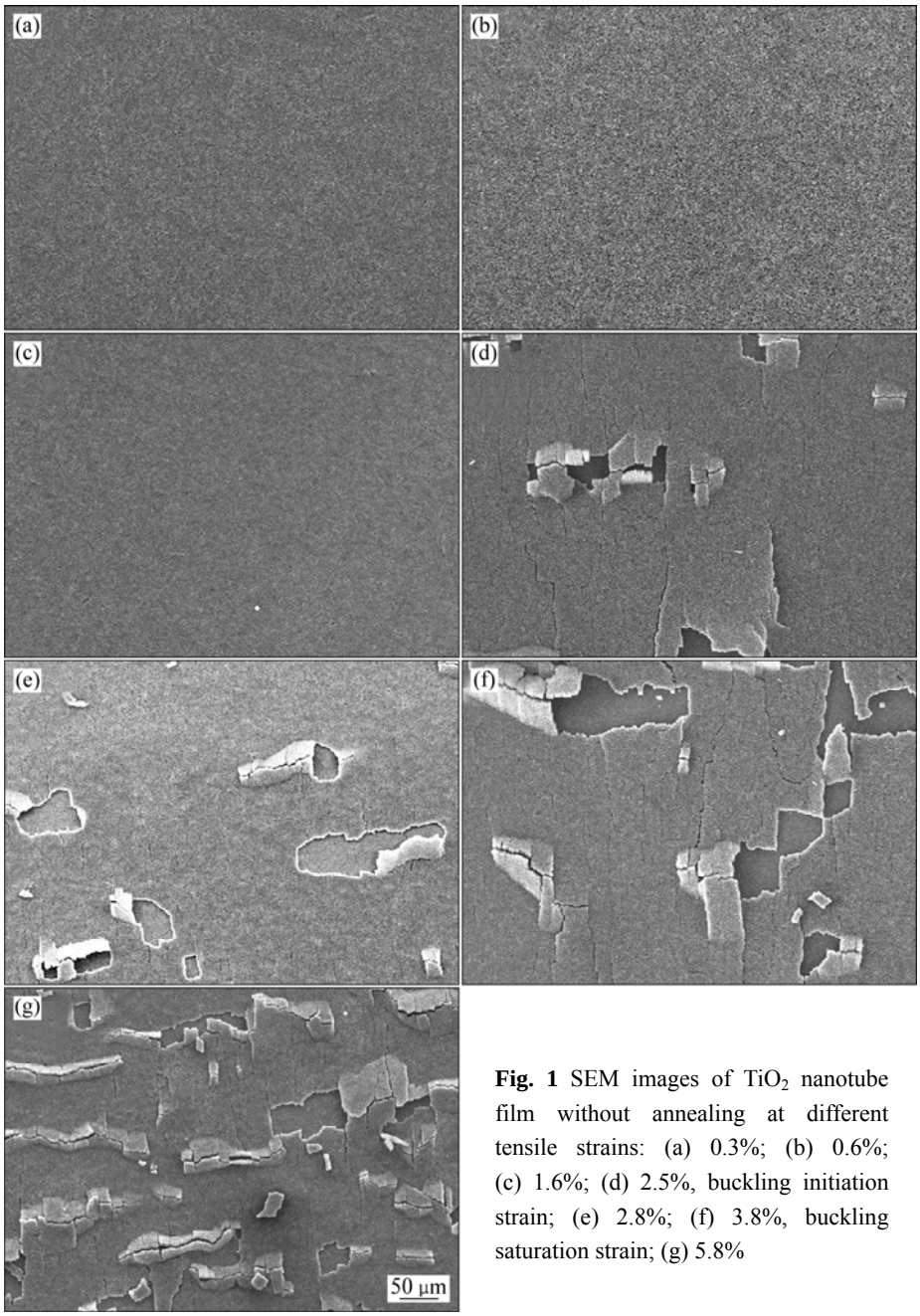

Fig. 1 SEM images of TiO_2 nanotube film without annealing at different tensile strains: (a) 0.3%; (b) 0.6%; (c) 1.6%; (d) 2.5%, buckling initiation strain; (e) 2.8%; (f) 3.8%, buckling saturation strain; (g) 5.8%

initiated, the propagation of buckling occurred rapidly within a narrow strain span (1.3% strain). Spallation happened simultaneously at the buckling initiation strain.

Buckling evolution of TiO_2 nanotube film with 250 °C annealing is shown in Fig. 2. The buckling initiation strain is 8.9% and the buckling saturation strain is 13.5%. A lot of tiny cracks occurred on the sample at buckling initiation. Spallation cannot be seen at the buckling initiation stage.

Buckling evolution of TiO_2 nanotube film with 400 °C annealing is given in Fig. 3. The buckling initiation strain is 7.8% and the buckling saturation strain is 12.2% (Fig. 3). Besides the buckling initiation, crack propagation occurred homogeneously at the buckling saturation stage. Spallation was not seen at the buckling initiation stage either.

Annealing was used to relieve or release the residual stress and to modify the interface of the film.

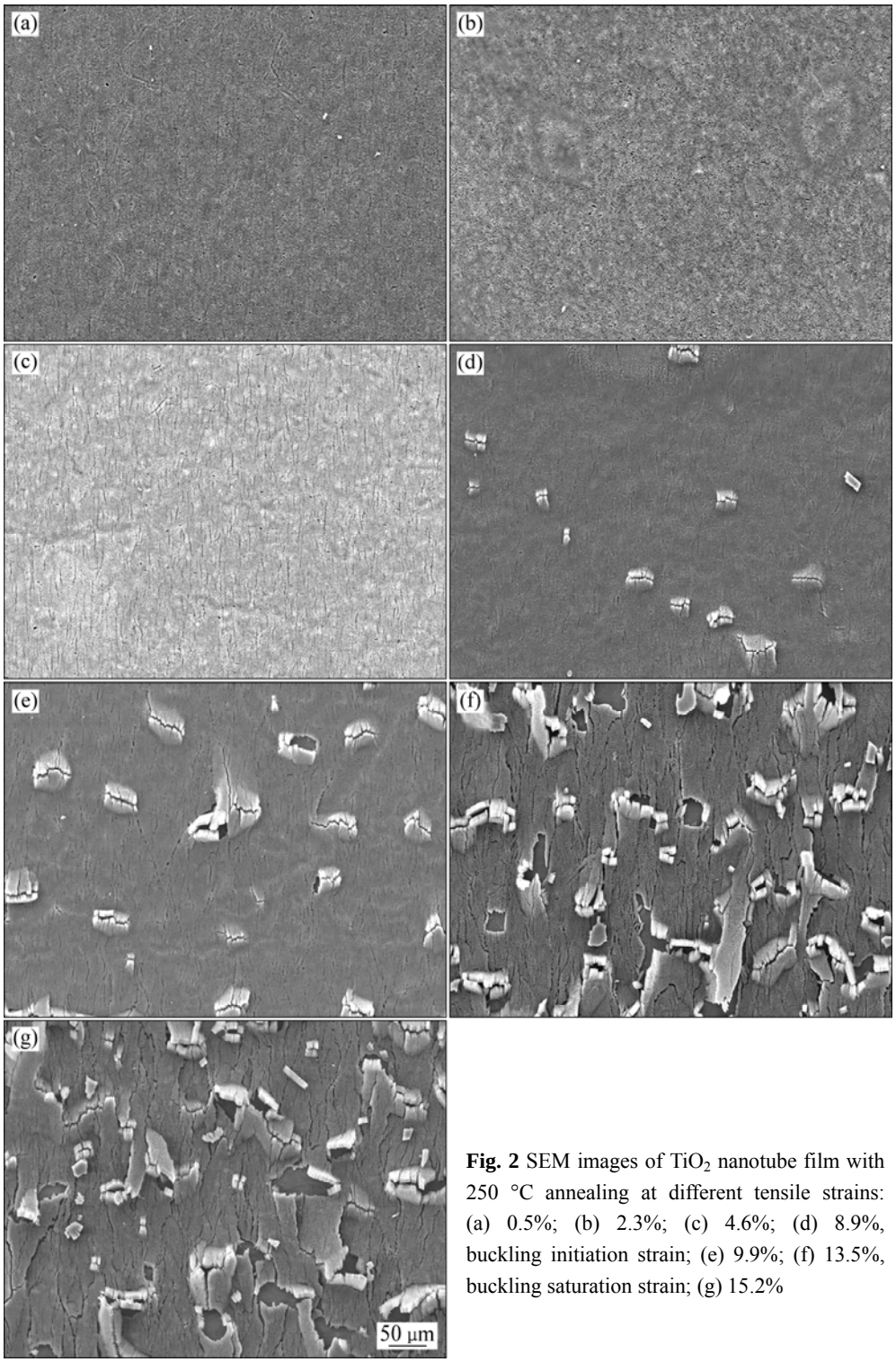

Fig. 2 SEM images of TiO_2 nanotube film with 250 °C annealing at different tensile strains: (a) 0.5%; (b) 2.3%; (c) 4.6%; (d) 8.9%, buckling initiation strain; (e) 9.9%; (f) 13.5%, buckling saturation strain; (g) 15.2%

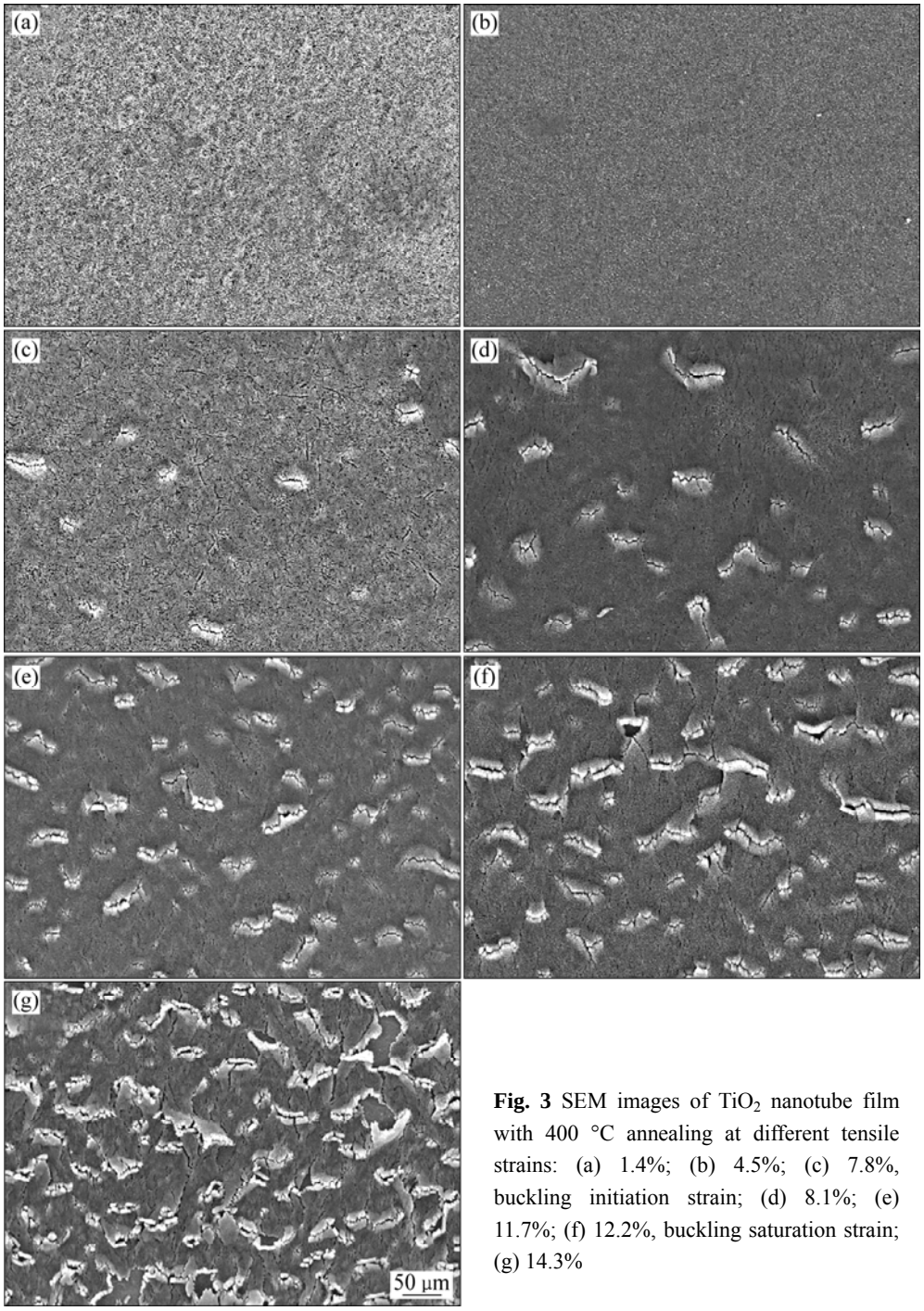

Fig. 3 SEM images of TiO_2 nanotube film with 400 °C annealing at different tensile strains: (a) 1.4%; (b) 4.5%; (c) 7.8%, buckling initiation strain; (d) 8.1%; (e) 11.7%; (f) 12.2%, buckling saturation strain; (g) 14.3%

The weaker the interface of the film/substrate, the easier the formation of the buckling and the spallation. The strains of buckling initiation of samples with 250 °C annealing and 400 °C annealing are much higher than those of room temperature samples. Spallation is not seen in 250 °C annealed and 400 °C annealed samples with buckling initiation, and spallation propagates rapidly after the buckling initiation in the samples without annealing. It can be concluded that 250 °C annealing and 400 °C annealing have obviously modified the interfacial properties of the TiO_2 nanotube film, which indicates excellent agreement with the crack analysis results [11].

The relationships between the buckle densities and the strains of the TiO_2 nanotube films are shown in Fig. 4. With the increase of tensile strain, buckle densities of TiO_2 nanotube films without annealing, with 250 °C annealing and with 400 °C annealing demonstrate the tendency of three processes including buckle initiation, buckle propagation and buckle saturation, which is consistent with the crack developing tendency [11]. The gap between the buckle initiation strain and the buckle

saturation strain is relatively narrow since the buckles propagate rapidly. At the buckle saturation stage, the buckle densities of TiO_2 nanotube films with 250 °C annealing and with 400 °C annealing are much larger compared with TiO_2 nanotube film without annealing. At the same time, the buckle density of TiO_2 nanotube film with 400 °C annealing is larger than that of TiO_2 nanotube film with 250 °C annealing. The reason is that temperature annealing has modified the interface of the TiO_2 nanotube film−Ti substrate and 400 °C annealing has better modifying effect than 250 °C annealing.

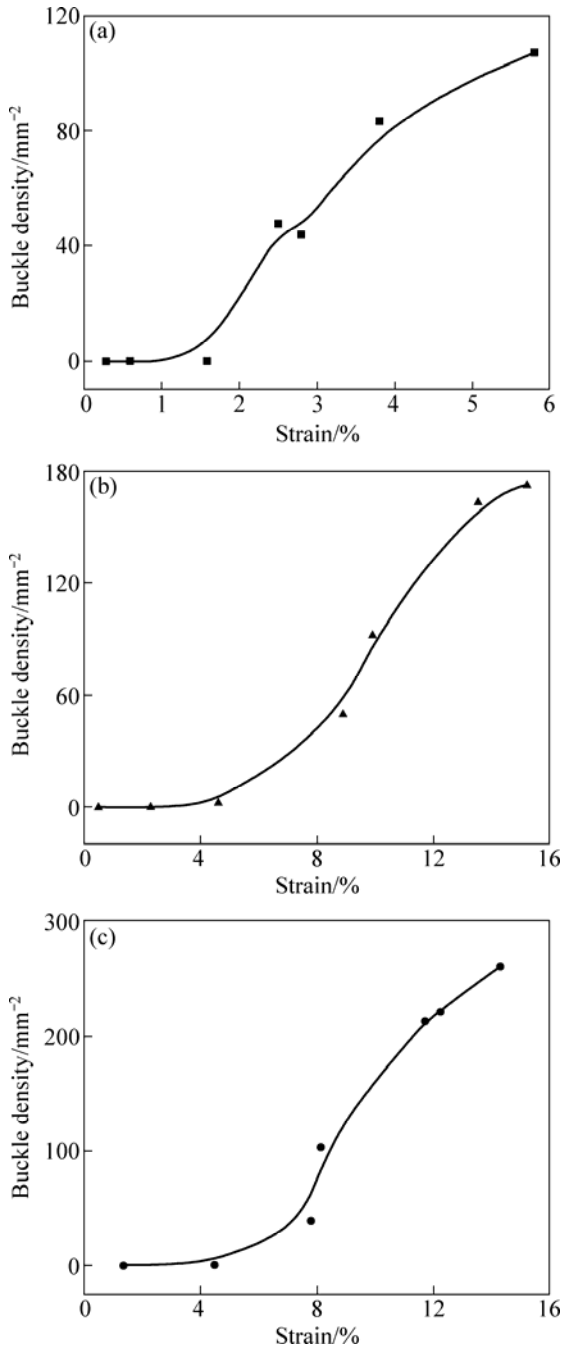

Fig. 4 Buckle densities as function of strain for TiO_2 nanotube films: (a) Without annealing; (b) With 250 °C annealing; (c) With 400 °C annealing

Under the loading of tensile stress, TiO_2 nanotube films will produce transverse cracks to dissipate the interfacial energies. When the energy generated by crack propagation is not enough to balance the increasing tensile energy, buckles occur. Furthermore, spallation occurs when the energy generated by buckle propagation is insufficient to consume the increasing tensile energy. Since the interface of TiO_2 nanotube film without annealing is the weakest, the spallation appears at its buckle initiation strain (Fig. 1(d)). For the TiO_2 nanotube films with 250 °C annealing and 400 °C annealing, spallation does not appear at their buckle initiation strain because of the interfacial modifying effect of temperature annealing. Spallation occurs at the buckle saturation strain for the TiO_2 nanotube film with 250 °C annealing (Fig. 2(f)). Even when the strain reaches the buckle saturation point for TiO_2 nanotube film with 400 °C annealing (Fig. 3(e)), spallation does not occur.

Based on the SEM images magnified with 200 times, the average half widths of the buckles at buckling initiation stage for TiO_2 nanotube films without annealing, with 250 °C annealing and with 400 °C annealing are 39.6, 26.3 and 21.4 μm, respectively.

According to Refs. [1,7,9,12], the buckling begins when the applied stress exceeds a critical value σ_c. The buckling appears randomly, probably due to the presence of defects. The theoretical value σ_c is given as:

$$\sigma_c = \frac{\pi^2}{12}\left(\frac{E_f}{1-\nu_f^2}\right)\left(\frac{a}{b}\right)^2 \quad (1)$$

where a is the film thickness; E_f is the elastic modulus of the film; υ_f is the Poisson ratio; b is the half width of the separation.

Therefore, the critical buckling stress of TiO_2 nanotube films without annealing, with 250 °C annealing and with 400 °C annealing can be estimated as 180.4, 410.2 and 619.5 MPa, respectively.

3.2 AFM buckling observation of TiO_2 nanotube film

Figure 5 shows an example of circular blister observed by AFM on TiO_2 nanotube film with 250 °C annealing at the buckling initiation strain of 8.9%. The scan rate is 0.5 Hz and the scan scope is about 60 μm×48.5 μm with a height extension of 7.5 μm.

For 250 °C annealed sample, the characteristics of the wrinkle are h=4.13 μm and b=24 μm. For the samples without annealing and with 400 °C annealing, the buckling heights are too large to be detected by AFM since AFM z limit is only 7.415 μm.

The critical buckling stress of TiO_2 nanotube films with 250 °C annealing by AFM observation is estimated as 470.2 MPa by equation (1), which indicates excellent

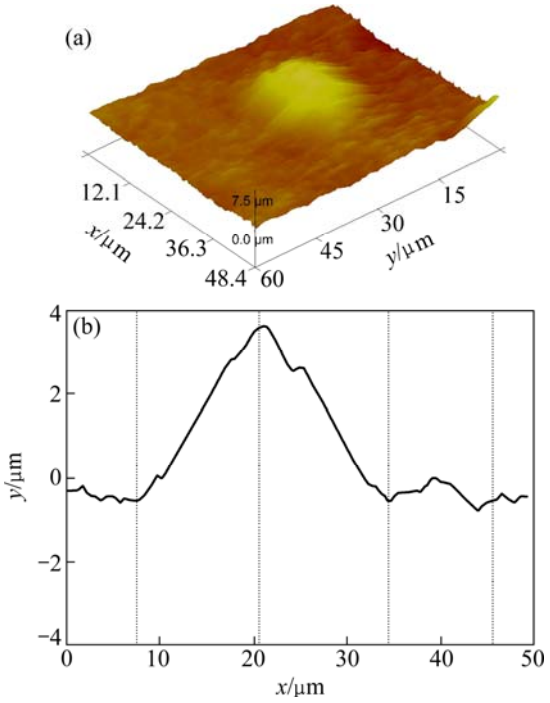

Fig. 5 Example of wrinkle observed by AFM on TiO_2 nanotube film with 250 °C annealing (a), same sample as Fig. 3(b) cross section of this wrinkle (b)

agreement with the critical buckling stress of TiO_2 nanotube films with 250 °C annealing by SEM observation (410.2 MPa).

The true stress of the film can be calculated according to equation (2) [9]:

$$\frac{h}{a}=[\frac{4}{3}(\frac{\sigma}{\sigma_c}-1)]^{1/2} \quad (2)$$

where h is the height of the wrinkle; a is the film thickness; σ is the true stress; σ_c is the critical buckling stress.

The true stress of 250 °C annealing sample can be estimated as 840.3 MPa.

Buckle formation can be seen in the substrate straining tensile test samples of TiO_2 nanotube film/titanium system. During tensile loading of the film, compressive transverse stresses arise in the film due to Poisson ratio mismatch between the substrate and the film. The compressive stress causes progressive buckling and delamination of film fragments transverse to the tensile loading direction [13].

The biaxial misfit thermal residual stress is defined accordingly as [14]:

$$\sigma_{thermal}=(\alpha_f-\alpha_s)(T-T_r)E_f/(1-\nu_s) \quad (3)$$

where T is the annealing temperature; T_r is the room temperature.

Thermal expansion coefficients of Ti and TiO_2 are 8.6×10^{-6} K^{-1} and 9×10^{-6} K^{-1}, respectively. So, the thermal residual stresses can be calculated as −14.1 MPa and −23.5 MPa for 250 °C annealed and 400 °C annealed samples, respectively. Therefore, the residual stress caused by thermal mismatch is compressive stress. The residual stress can be neglected compared with the critical buckling stresses of the TiO_2 nanotube film since it is very low.

The structural mismatch-induced stress is internal residual stress, which comes from the difference in crystal structure between the film and the substrate as well as lattice distortion within the film as a result of defects or incorporation of foreign molecules. It can be measured by the radius of the curvature of the film [3].

The interfacial toughness of the film can be explained by the critical energy release rate. The critical energy release (G_c) rate is calculated as [6]:

$$G_c=[\frac{(1-\nu^2)a}{2E}](\sigma-\sigma_c)(\sigma+3\sigma_c) \quad (4)$$

Therefore, the critical energy release rate of 250 °C annealed sample was calculated as 77.2 J/m^2.

According to AGRAWAL and RAJ's interfacial shear strength model [1] and BEUTH's energy release rate equation [15], the critical energy release rate of TiO_2 nanotube film with 250 °C annealing was calculated as 102.6 J/m^2 on the basis of crack density at saturation [11]. Hereby, excellent agreement of the critical energy release rate of TiO_2 nanotube film with 250 °C annealing has been obtained. The estimated results both from buckling and crack consideration are convincible.

4 Conclusions

1) Annealing temperature demonstrates modifying effects on the interface of TiO_2 nanotube film-titanium substrate. TiO_2 nanotube films without annealing, with 250 °C annealing and with 400 °C annealing demonstrate the tendency of three processes including buckle initiation, buckle propagation and buckle saturation, which indicates excellent agreement with the crack developing tendency.

2) Through SEM observation, the critical buckling stresses of TiO_2 nanotube films without annealing, with 250 °C annealing and 400 °C annealing were estimated as 180, 410 and 619.5 MPa, respectively. The critical buckling stress of TiO_2 nanotube film with 250 °C annealing was calculated as 470 MPa by AFM observation, which shows good response to the results by SEM observation.

3) The critical energy release rate of TiO_2 nanotube film with 250 °C annealing was obtained as 77.2 J/m^2, which shows good agreement with the energy release rate for TiO_2 nanotube film with 250 °C annealing (102.6 J/m^2).

Acknowledgements

The authors express their sincere thanks to Dr. EBACHER Vincent and Mr. MA Menghan for the technical support during the course of this work.

References

[1] AGRAWAL D C, RAJ R. Measurement of the ultimate shear strength of a metal-ceramic interface [J]. Acta Metallurgy, 1989, 37(4): 1265−1270.

[2] YANG B Q, ZHANG K, CHEN G N, LUO G X, XIAO J H. Measurement of fracture toughness and interfacial shear strength of hard and brittle Cr coating on ductile steel substrate [J]. Surface Engineering, 2008, 24(5): 332−336.

[3] ZHANG S, WANG Y S, ZENG X T, CHENG K, QIAN M, SUN D E, WENG W J, CHIA W Y. Evaluation of interface shear strength and residual stress of sol−gel derived fluoridated hydroxyapatite coatings on Ti6Al4V substrates [J]. Engineering Fracture Mechanics, 2007, 74: 1884−1893.

[4] FRANK S, HANDQE U A, OLLIQES S, SPOLENAK R. The relationship between thin film fragmentation and buckle formation: Synchrotron-based in situ studies and two-dimensional stress analysis [J]. Acta Materialia, 2009, 57(5): 1442−1453.

[5] WANG J S, EVANS A G. Measurement and analysis of buckling and buckle propagation in compressed oxide layers on superalloy substrates [J]. Acta Materialia, 1998, 46(14): 4993−5005.

[6] JENSEN H M, SHEINMAN I. Straight sided, buckling-driven delamination of thin films at high stress levels [J]. International Journal of Fracture, 2001, 110(4): 371−385.

[7] TALEA M, BOUBEKER B, CLEYMAND F, COUPEAU C, GRILHE C, GOUDEAU P H. Atomic force microscopy observations of debonding in 304L stainless steel thin steel [J]. Materials Letters, 1999, 41: 181−185.

[8] BRANGER V, COUPEAU C H, GOUDEAU P H. Atomic force microscopy analysis of buckling phenomena in metallic thin films on substrates [J]. Journal of Materials Science Letters, 2000, 19: 353−355.

[9] PARRY G, COLIN J, COUPEAU C, FOUCHER F, CIMETIERE A, GRILHE J. Effect of substrate compliance on the global unilateral post-buckling of coatings: AFM observations and finite element calculations [J]. Acta Materialia, 2005, 53: 441−447.

[10] DENG B Y, YAN X, WEI Q F, GAO W D. AFM characterization of nonwoven material functionalized by ZnO sputter coating [J]. Materials Characterization, 2007, 58: 854−858.

[11] ZOU Jian-peng, WANG Ri-zhi. Crack initiation, propagation and saturation of TiO_2 nanotube film [J]. Transactions of Nonferrous Metals Society of China, 2012, 22(3): 627−633.

[12] HUTCHISON J W, THOULESS M D, LINIGER E G. Growth and configurational stability of circular, buckling-driven film delaminations [J]. Acta Metallurgica et Materialia, 1992, 40(2): 295−308.

[13] ANDERSONS J, TARASOVS Y, LETERRIER Y. Evaluation of thin film adhesion to a compliant substrate by the analysis of progressive buckling in the fragmentation test [J]. Thin Solid Films, 2009, 517: 2007−2011.

[14] WATANABE M. Measurement of the residual stress in a Pt-aluminide bond coat [J]. Scripta Materialia, 2002, 46(1): 67−70.

[15] BEUH J L Jr. Cracking of thin bonded films in residual tension [J]. International Journal of Solids Structures, 1992, 29(13): 1657−1675.

TiO_2 纳米管薄膜的屈曲图样

邹俭鹏[1]，WANG Ri-zhi[2]

1. 中南大学 粉末冶金国家重点实验室，长沙 410083；

2. Department of Materials Engineering, University of British Columbia, Vancouver BC, V6T 1Z4, Canada

摘　要：采用基体应变测试方法研究 TiO_2 纳米管薄膜的屈曲图样。结果表明：TiO_2 纳米管薄膜室温样、250 ℃退火样和 400 ℃退火样的屈曲应变依次为 2.5%、8.9% 和 7.8%，说明退火改善了纳米管薄膜/Ti 基体界面状况。从 SEM 观察可以看出，TiO_2 纳米管薄膜室温样、250 ℃退火样和 400 ℃退火样的临界屈曲应力分别为 180.4、410.2 和 619.5 MPa；从 AFM 观察可以看出，TiO_2 纳米管薄膜 250 ℃退火样的临界屈曲应力为 470.2 MPa，两者吻合得很好。采用 AFM 计算 250 ℃退火样的真实应力和能量释放率分别为 840.3 MPa 和 77.2 J/m^2，此结果与从裂纹角度计算出的 250 ℃退火样的能量释放率 102.6 J/m^2 吻合得很好。

关键词：TiO_2 纳米管；阳极氧化；屈曲；能量释放率

(Edited by LI Xiang-qun)